

## Conference Paper

# Optical Properties of $\text{Cu}_2\text{S}/\text{SnS}_2$ Precursor Layers for the Preparation of Kesterite $\text{Cu}_2\text{SnS}_3$ Photovoltaic Absorber

L. N. Maskaeva<sup>1,2</sup>, O. A. Lipina<sup>3</sup>, V. F. Markov<sup>1,2</sup>, E. A. Fedorova<sup>1</sup>, and E. A. Klochko<sup>1</sup>

<sup>1</sup>Ural Federal University, 620002 Ekaterinburg, Russia

<sup>2</sup>Ural Institute of State Fire Service of EMERCOM of Russia, 620022 Ekaterinburg, Russia

<sup>3</sup>Institute of Solid State Chemistry, UB RAS, Ekaterinburg, Russia

## Abstract

The  $\text{Cu}_2\text{S}$  and  $\text{SnS}_2$  layers have been prepared by the chemical bath deposition method. The results of SEM and EDX analyses confirm a high stoichiometry of the synthesized semiconductor thin films. The optical properties of the  $\text{Cu}_2\text{S}$  and  $\text{SnS}_2$  layers have been studied, and the optical band gap values have been determined.

**Keywords:** thin films, sulfides, band gap, hydrochemical deposition, transmittance, photovoltaic absorber

Corresponding Author:

O. A. Lipina

LipinaOlgaA@yandex.ru

Received: 14 September 2018

Accepted: 1 October 2018

Published: 14 October 2018

Publishing services provided by  
Knowledge E

© L. N. Maskaeva et al. This article is distributed under the terms of the [Creative Commons Attribution License](#), which permits unrestricted use and redistribution provided that the original author and source are credited.

Selection and Peer-review under the responsibility of the ASRTU Conference Committee.

## 1. Introduction

Thin film solar cells attract much attention due to their low cost, high stability and efficiency. Most of the research is focused on *p*-type semiconductor  $\text{Cu}(\text{In,Ga})(\text{S/Se})_2$  and  $\text{CdTe}$  absorber layers. The efficiency of solar cell power conversion of chalcopyrite based  $\text{Cu}(\text{In,Ga})\text{Se}_2$  thin films can reach 22% [1]. However, the abovementioned compounds consist of toxic and rare elements that limits their use in large-scale mass production.

Recently, some ternary compounds in Cu-Sn-S system, namely  $\text{Cu}_2\text{SnS}_3$ ,  $\text{Cu}_2\text{Sn}_3\text{S}_7$ ,  $\text{Cu}_3\text{SnS}_4$ ,  $\text{Cu}_4\text{SnS}_4$ ,  $\text{Cu}_4\text{SnS}_5$ , and  $\text{Cu}_4\text{Sn}_7\text{S}_{16}$  have been offered as possible candidates for photovoltaic applications [2–4]. Among the listed sulfides,  $\text{Cu}_2\text{SnS}_3$  (CTS) is considered to be the most promising absorber material due to its chemical and thermal stability; moreover, its constituents are earth abundant and non-toxic. The band gap of this semiconductor depends on the crystal structure and varies from 0.93 to 1.51 eV [4–6]. To date, the maximum value of power conversion efficiency in a  $\text{Cu}_2\text{SnS}_3$  thin film solar

## OPEN ACCESS

cell is 4.8% [7]. Although this value is less than those for  $\text{Cu}(\text{In,Ga})\text{Se}_2$  (~22%),  $\text{CuInS}_2$  (11.4%), and  $\text{Cu}_2\text{ZnSnS}_x\text{Se}_{4-x}$  (12.6%) [1, 8, 9], there are different ways to increase the  $\text{Cu}_2\text{SnS}_3$  solar cells performance, for example, the use of  $\text{In}_2\text{S}_3$  as a buffer layer [10] or incorporation of alkalis (Na, Li, or K) [11, 12].

There are various techniques for the preparation of  $\text{Cu}_2\text{SnS}_3$  thin film [2, 7, 8, 11, 12]. One of them is an annealing process under a sulfur atmosphere from sandwich layers of  $\text{Cu}_2\text{S}$  and  $\text{SnS}_2$ . This method is based on the mobility of copper in copper sulfide films [13], which allows  $\text{Cu}_2\text{SnS}_3$  to be synthesized after appropriate heat treatment of  $\text{Cu}_2\text{S}/\text{SnS}_2$  stacked precursor layers. In this work,  $\text{Cu}_2\text{S}$  and  $\text{SnS}_2$  precursor layers were prepared by the chemical bath deposition method. The morphological characteristics of the films were studied. Special attention was paid to the investigation of the optical properties of precursor layers; the obtained results were compared with the available literature data.

## 2. Methods

$\text{Cu}_2\text{S}$  and  $\text{SnS}_2$  layers were prepared by the chemical bath deposition method. The  $\text{Cu}_2\text{S}$  layer was synthesized from the solution of  $\text{CuCl}_2$  and  $\text{Na}_2\text{SO}_3$ . The latter acted as a ligand slowing down the speed of metal sulfide formation. The tartaric acid ( $\text{C}_4\text{H}_6\text{O}_6$ ) was added to provide a weak acid environment. The reducing environment for  $\text{Cu}^{2+}$  to  $\text{Cu}^+$  transfer was provided by introduction of hydroxylamine hydrochloride ( $\text{NH}_2\text{OH}\cdot\text{HCl}$ ) having a rather high value of redox potential ( $\varphi_{\text{NH}_3\text{OH}^+/\text{N}_2} = -1.87 \text{ V}$ ). In the case of  $\text{SnS}_2$ , the synthesis was carried out from the solution of tin chloride ( $\text{SnCl}_2$ ) and sodium thiosulphate ( $\text{Na}_2\text{S}_2\text{O}_3$ ). Sodium citrate ( $\text{Na}_3\text{C}_6\text{H}_5\text{O}_7$ ) was used as a reagent regulating the content of active  $\text{Sn}^{2+}$  ions in the reaction mixture. The deposition was carried out for 120 minutes at 343 K in sealed reactors made of molybdenum glass, in which fat-free glasses or siall substrates were fixed using the teflon holders. The reactors were placed in a TS-TB-10 thermostat, providing the accuracy of temperature maintenance  $\pm 1 \text{ K}$ .

The morphology and elemental composition of the samples were studied using a JEOL JSM-5900 LV scanning electron microscope (SEM) equipped with an EDS IncaEnergy 250 energy-dispersive X-ray detector. The transmittance spectra were recorded in the interval of 200–1850 nm on a Shimadzu UV-3600 UV-VIS-NIR spectrophotometer.

### 3. Results

Figure 1 shows the SEM images of the  $\text{Cu}_2\text{S}$  and  $\text{SnS}_2$  thin films freshly deposited on sital substrates. The results of SEM and EDX analyses confirm a high stoichiometry of the synthesized semiconductor layers. In case of  $\text{Cu}_2\text{S}$ , the concentration of copper and sulfur is  $62.86 \pm 1.0$  and  $31.43 \pm 1.0$  at.%, respectively, both in separate particles and in interphase surfaces of the film. A small amount of chlorine (5.71 at.%) is also found in the deposited  $\text{Cu}_2\text{S}$  precursor layer that is caused by the capture of chloride ions from the reaction mixture containing  $\text{CuCl}_2$  and  $\text{NH}_2\text{OH HCl}$ . Both films are formed from particles of 50–200 nm in size.

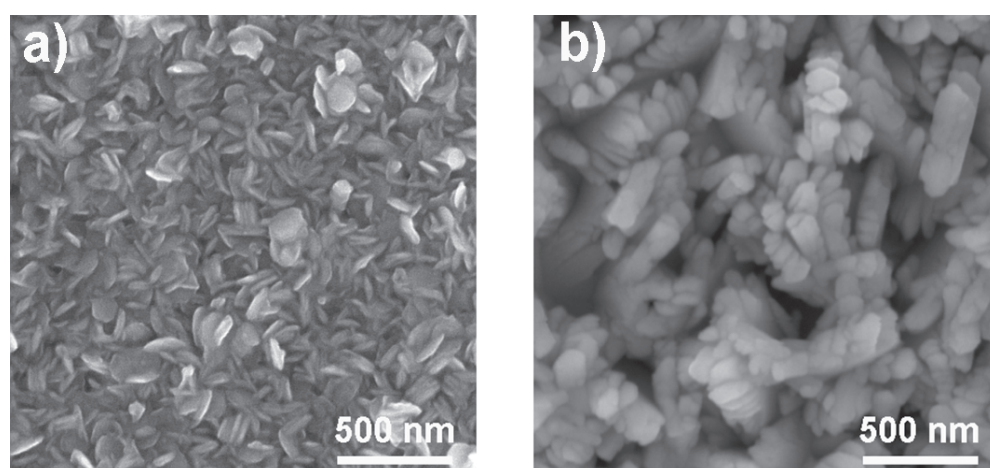


**Figure 1:** SEM images of (a)  $\text{Cu}_2\text{S}$  and (b)  $\text{SnS}_2$  precursor layers deposited on sital substrates, 100000x magnification.

The spectral transmittance curves of  $\text{Cu}_2\text{S}$  and  $\text{SnS}_2$  thin films are presented in Figure 2(a). The fundamental absorption onsets are observed at 420–800 and 800–1150 nm, respectively, which coincides with the reported values for these phases. The optical absorption data were analyzed to determine the optical bandgap values using the Tauc relation [14]:

$$\alpha h\nu = C(h\nu - E_g)^n \quad (1)$$

where  $\alpha$  is the absorption coefficient of material,  $h\nu$  is the photon energy,  $C$  is the proportionality constant,  $E_g$  is the optical band gap, and  $n$  is a constant associated with different types of electronic transitions ( $n = 1/2$  for direct allowed transition,  $n = 2$  for indirect allowed one,  $n = 3/2$  for direct forbidden one, and  $n = 3$  for indirect forbidden one).

The optical absorption coefficient ( $\alpha$ ) was calculated by the equation:

$$\alpha = (1/t) \ln(1/T) \quad (2)$$

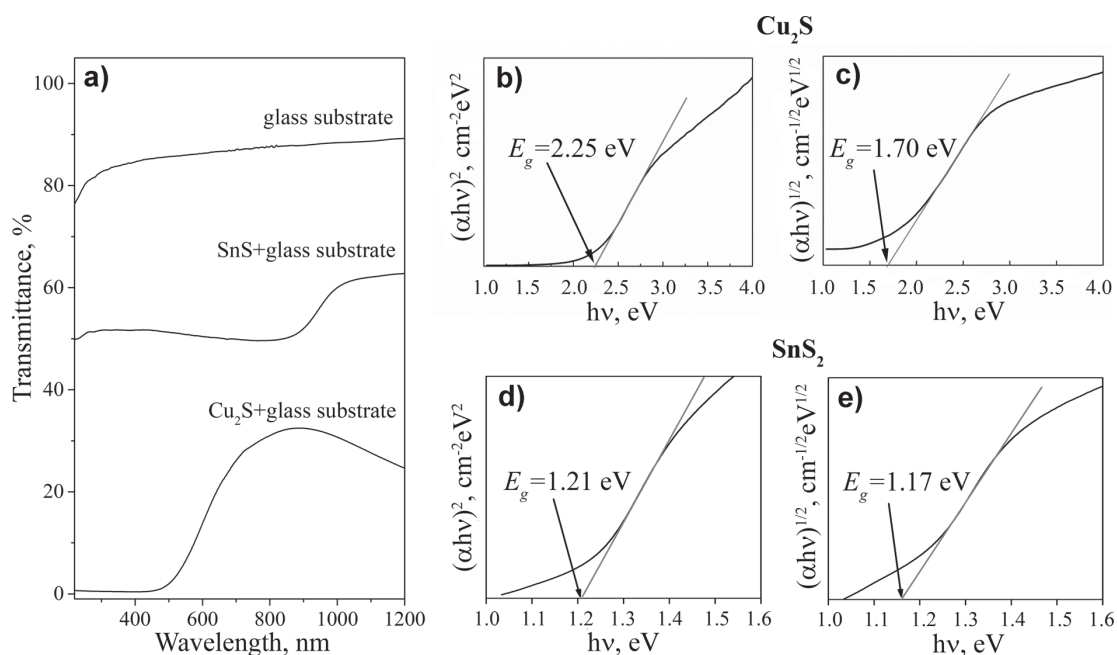


**Figure 2:** (a) Transmittance spectra of Cu<sub>2</sub>S and SnS<sub>2</sub> thin films deposited on glass substrates. Determination of the band gap energies of the layers in the approximation of (b) & (d) direct allowed and (c) & (e) indirect allowed transitions.

where  $T$  is the transmittance of the film and  $t$  is the film thickness (in our case  $t = 200$  nm).

Appropriate functions  $[\alpha h\nu]^{1/n}$  versus  $h\nu$  were plotted. Since there is a discrepancy in the type of transitions in Cu<sub>2</sub>S and SnS<sub>2</sub> compounds, we estimated  $E_g$  taking into account a direct and indirect allowed transitions; four functions (with  $n = 1/2$  and  $n = 2$ ) were studied. The results of the fitting procedure of the linear parts are presented in Figure 2(b)–(e). It is seen that the curves characterizing the two different types of transitions have wide linear regions, indicating that the direct as well as indirect bandgap relations are applicable.

The calculated  $E_g$  value for the Cu<sub>2</sub>S thin film is equal to 2.25 eV and 1.70 eV for the direct and indirect transition types, respectively. These bandgap energies are consistent with the reported values of 1.1–2.2 eV for Cu<sub>2</sub>S films [4, 15, 16]. In case of SnS<sub>2</sub> layer, the bandgap energy values are 1.21 eV and 1.17 eV for the direct and indirect transitions, in agreement with the literature data (0.81–3.38 eV) [17, 18]. The wide spread of the published values may be caused by the deviation from ideal stoichiometry and by differences in the techniques and conditions of Cu<sub>2</sub>S and SnS<sub>2</sub> thin films preparation. The SnS<sub>2</sub> precursor layer synthesized in this work can be used for photovoltaic applications, because its indirect bandgap of 1.17 eV is close to the energy band gap for optimum solar absorbing material (1.1 eV) [4].

## 4. Conclusion

The  $\text{Cu}_2\text{S}$  and  $\text{SnS}_2$  layers prepared by chemical bath deposition have been studied. Both films have homogeneous chemical composition and are formed from particles of 50–200 nm in size. According to the transmittance spectroscopy data, the  $\text{Cu}_2\text{S}$  and  $\text{SnS}_2$  samples begin to absorb light at wavelengths less than 1150 nm and 800 nm, respectively. The band gap energies determined in the approximation of direct allowed types of transitions are equal to 2.25 eV and 1.21 eV for  $\text{Cu}_2\text{S}$  and  $\text{SnS}_2$  thin films, respectively. These precursor layers may be successfully used for growing kesterite  $\text{Cu}_2\text{SnS}_3$  photovoltaic absorber.

## Funding

The work was financially supported by program 211 of the Government of the Russian Federation (No. 02.A03.21.0006) and by the FASO program No. AAAA-A16-116122810218-7.

## References

- [1] Jackson, P., Wuerz, R., Hariskos, D., et al. (2016). Effects of heavy alkali elements in  $\text{Cu}(\text{In,Ga})\text{Se}_2$  solar cells with efficiencies up to 22.6%. *Physica Status Solidi RRL*, vol. 10, pp. 583–586.
- [2] Nakashima, M., Yamaguchi, T., Itani, H., et al. (2015).  $\text{Cu}_2\text{SnS}_3$  thin film solar cells prepared by thermal crystallization of evaporated Cu/Sn precursors in sulfur and tin atmosphere. *Physica Status Solidi C*, vol. 12, pp. 761–764.
- [3] Zawadzki, P., Baranowski, L. L., Peng, H. W., et al. (2013). Evaluation of photovoltaic materials within the Cu–Sn–S family. *Applied Physics Letters*, vol. 103, p. 253902.
- [4] Fu, H. (2018). Environmental-friendly and earth-abundant colloidal chalcogenide nanocrystals for photovoltaics applications. *Journal of Materials Chemistry C*, vol. 6, pp. 414–445.
- [5] Avellaneda, D., Nair, M. T. S., and Nair, P. K. (2010).  $\text{Cu}_2\text{SnS}_3$  and  $\text{Cu}_4\text{SnS}_4$  thin films via chemical deposition for photovoltaic application. *Journal of the Electrochemical Society*, vol. 157, pp. D346–D352.
- [6] Berg, D. M., Djemour, R., Gütay, L., et al. (2012). The film solar cells based on the ternary compound  $\text{Cu}_2\text{SnS}_3$ . *Thin Solid Films*, vol. 520, pp. 6291–6294.

- [7] Nakashima, M., Fujimoto, J., Yamaguchi, T., et al. (2015).  $\text{Cu}_2\text{SnS}_3$  thin film solar cells fabricated by sulfurization from NaF/Cu/Sn stacked precursor. *Applied Physics Express*, vol. 8, p. 42303.
- [8] Braunger, D., Hariskos, D., Walter, T., et al. (1996). Sequential processes for the deposition of polycrystalline  $\text{Cu}(\text{In,Ga})(\text{S,Se})_2$  thin films: Growth mechanism and devices. *Solar Energy Materials and Solar Cells*, vol. 40, pp. 97–102.
- [9] Wang, W., Winkler, M. T., Gunawan, O., et al. (2014). Device characteristics of CZTSSe thin-film solar cells with 12.6% efficiency. *Advanced Energy Materials*, vol. 4, p. 1301465.
- [10] Chen, Q., Dou, X., Ni, Y., et al. (2012). Study and enhance the photovoltaic properties of narrow-bandgap  $\text{Cu}_2\text{SnS}_3$  solar cell by p-n junction interface modification. *Journal of Colloid and Interface Science*, vol. 376, pp. 327–330.
- [11] Nakashima, M., Fujimoto, J., Yamaguchi, T., et al. (2017). KF addition to  $\text{Cu}_2\text{SnS}_3$  thin films prepared by sulfurization process. *Japanese Journal of Applied Physics*, vol. 56, pp. 2C–4C.
- [12] Ruan, C., Tao, J., Zhu, C., et al. (2018). Effect of potassium doping for ultrasonic sprayed  $\text{Cu}_2\text{SnS}_3$  thin films for solar cell application. *Journal of Materials Science: Materials in Electronics*. Retrieved from <https://doi.org/10.1007/s10854-018-9401-9>
- [13] Amlouk, M., Dachraoui, M., Belgacem, S., et al. (1987). Structural, optical and electrical properties of  $\text{SnO}_2\text{:F}$  and CdS airless sprayed layers. *Solar Energy Materials and Solar Cells*, vol. 15, pp. 453–461.
- [14] Tauc, J. and Abeles, F. (1970). *Optical Properties of Solids*. Amsterdam: IOP Publishing Ltd.
- [15] Mulder, B. J. (1973). Optical properties of an unusual form of thin chalcosite ( $\text{Cu}_2\text{S}$ ) crystals. *Physica Status Solidi A*, vol. 15, pp. 409–413.
- [16] Ramya, M. and Ganesan, S. (2013). Influence of thickness and temperature on the properties of  $\text{Cu}_2\text{S}$  thin films. *Iranian Journal of Science and Technology*, vol. 37A3, pp. 293–300.
- [17] Acharya, S. and Srivastava, O. N. (1981). Electronic behaviour of  $\text{SnS}_2$  crystals. *Physica Status Solidi A*, vol. 65, pp. 717–723.
- [18] Zhu, X., Luo, X., Yuan, H., et al. (2018). Band gap engineering of  $\text{SnS}_2$  nanosheets by anion-anion codoping for visible-light photocatalysis. *RSC Advances*, vol. 8, pp. 3304–3311.